Spin pumping in an altermagnet/normal-metal bilayer

Erik Wegner Hodt * and Jacob Linder

Center for Quantum Spintronics, Department of Physics, Norwegian University of Science and Technology, NO-7491 Trondheim, Norway

(Received 13 October 2023; revised 5 April 2024; accepted 30 April 2024; published 23 May 2024)

Altermagnetism is a subclass of antiferromagnetism that features spin-polarized electron bands of a nonrelativistic origin despite the absence of net magnetization in the material. We here theoretically study spin pumping from an altermagnetic insulator into a normal metal. The symmetry properties of the lattice and spin order of the altermagnet alter the magnon dispersion compared to a conventional square lattice antiferromagnet. We find that for a homogeneous magnetic field, the spin pumping current is the same as that of a regular antiferromagnet. If, however, the magnetic field becomes spatially dependent, we predict that the altermagnetic order will leave a unique fingerprint on the spin pumping behavior when the orientation of the spatial modulation does not align with the high-symmetry paths of magnon degeneracy in the altermagnet. This demonstrates that altermagnets can be used for terahertz spin pumping purposes with novel behavior, distinguishing them from their regular antiferromagnet counterparts.

DOI: 10.1103/PhysRevB.109.174438

I. INTRODUCTION

Injecting spins into materials is an important concept in the research field of spintronic devices [1]. Such an injection can be achieved in different ways, such as applying a spin-polarized electric current or via spin pumping. The spin pumping technique [2,3] consists of setting the spins in a magnetic material into precessional motion, which causes the material to emit a flow of spin into an adjacent material. By varying which material the spins are pumped into, the spin current can be modified depending on the material properties. Moreover, the absorption of the spin current can provide useful information about the band structure and spin-dependent interactions in the material receiving the spin current. However, one can also vary the material from which the spin current is pumped. Spin pumping is possible using both ferromagnetic [2,4] and antiferromagnetic materials [5,6], metals as well as insulators.

Recently, a class of antiferromagnetic materials known as altermagnets has sparked much interest in the research community [7–10]. These materials have features in common with both ferromagnets and antiferromagnets [11–13]. Similar to conventional collinear antiferromagnets, they break time reversal symmetry but have no net magnetization because the time-reversal operation can be nullified by an appropriate lattice transformation. In antiferromagnets this is a lattice translation operation while it is a lattice rotation in altermagnets. However, in contrast to such materials but similar to ferromagnets, altermagnets feature spin-polarized electron bands. This requires $\mathcal{PT}$-symmetry breaking, where $\mathcal{P}$ is the parity operation and $\mathcal{T}$ is the time-reversal operation. This also modifies the magnon dispersion relation compared to conventional antiferromagnets [14,15]. Predictions for altermagnetic materials span a range of different materials: insulators like FeF_2 and MnF_2, semiconductors like MnTe, metals like RuO_2, and superconductors like La_2CuO_4 [11,16–18].

In this work, we study spin pumping from an altermagnetic insulator into a normal metal using a nonequilibrium Keldysh Green's function perturbation technique. The altermagnet is described using the model in Ref. [14], featuring two intercalated square sublattices with a spin order that breaks $\mathcal{PT}$ symmetry. We find that the spin current pumped from the altermagnet is equal to the spin current pumped from a conventional square lattice antiferromagnet with Néel order when the magnetic field is homogeneous. This can change if the magnetic field used to set the altermagnetic spins into precessional motion is spatially inhomogeneous. Depending on the orientation of the spatial modulation of the magnetic field, the field can couple to degenerate or nondegenerate magnons in the altermagnet, giving rise to novel spin pumping behavior in the terahertz regime. Our findings predict that it should be possible to obtain a unique spin pumping signature from an altermagnet/normal-metal system which distinguishes it from a regular system based on an antiferromagnet.

II. MODEL

We consider a system consisting of an altermagnetic insulator (AM) coupled to a normal metal (NM) through an interface, described by an exchange term in the Hamiltonian. The setup is presented schematically in Fig. 1. The Hamiltonian in question is given by

$$H = H_{\mathrm{AM}} + H_{\mathrm{N}} + H_{\mathrm{int}}, \tag{1}$$

where the altermagnetic insulator term is given by the effective, symmetry-determined Hamiltonian

$$H_{\mathrm{AM}} = J_1 \sum_{\langle i,j\rangle} \hat{\mathbf{S}}_{Ai} \cdot \hat{\mathbf{S}}_{Bj} + J_2 \sum_{\langle i,j\rangle \in d_1} \hat{\mathbf{S}}_{Ai} \cdot \hat{\mathbf{S}}_{Aj} + J_2' \sum_{\langle i,j\rangle \in d_2} \hat{\mathbf{S}}_{Ai} \cdot \hat{\mathbf{S}}_{Aj} + K \sum_i \left(\hat{S}^z_{Ai}\right)^2$$

*Corresponding author: erik.w.hodt@ntnu.no

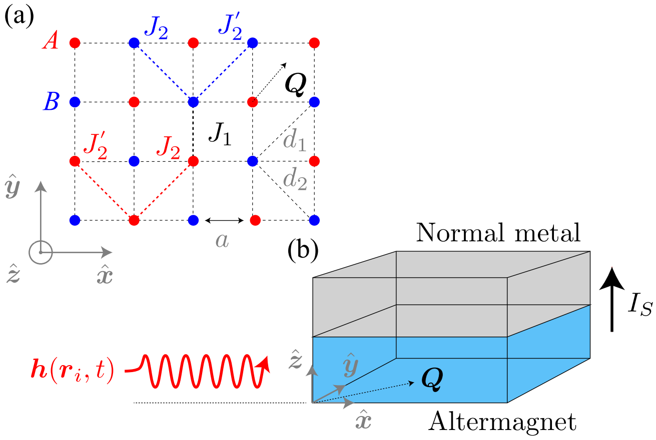

FIG. 1. Schematic overview of the altermagnetic insulator/normal-metal bilayer setup. (a) The effective, symmetry-determined altermagnetic insulator (AM) Hamiltonian contains three exchange coefficients in addition to an easy-axis anisotropy coupling K. The regular Heisenberg coupling $J_1 > 0$ favors an antiferromagnetic coupling between the different sublattices (red and blue), while the intrasublattice coefficients $J_2 < 0$ and $J_2' < 0$ favor a spatially anisotropic tendency towards ferromagnetic alignment within a sublattice. For the two sublattices, J_2 and J_2' act along opposite diagonals d_1 and d_2. a is the lattice parameter. $\boldsymbol{Q}$ is the modulation vector determining the spatial modulation of the magnetic field. It lies generally in the xy plane and is introduced in Eq. (3). (b) The bilayer setup showing how a spin current is established across the AM-NM interface by an external magnetic field causing precession of the magnetization in the AM.

$$+J_2' \sum_{\langle i,j\rangle \in d_1} \hat{\mathbf{S}}_{Bi} \cdot \hat{\mathbf{S}}_{Bj} + J_2 \sum_{\langle i,j\rangle \in d_2} \hat{\mathbf{S}}_{Bi} \cdot \hat{\mathbf{S}}_{Bj}$$
$$+ K \sum_i \left(\hat{S}^z_{Bi}\right)^2 - \zeta \sum_i \hat{\mathbf{S}}_i \cdot \boldsymbol{h}(\boldsymbol{r}_i, t). \qquad (2)$$

Here, A and B denote the two distinct sublattices of the square lattice in the altermagnet and the spin operator $\hat{\mathbf{S}}_{Ai}$ corresponds to a localized spin on site i residing in the A sublattice. As for the various exchange coefficients, $J_1 > 0$ describes the regular Heisenberg exchange between nearest-neighbor spins on opposite sublattices, favoring an antiparallel spin configuration of the sublattices. $J_2 < 0$ and $J_2' < 0$ govern a ferromagnetic and spatially anisotropic intrasublattice exchange coupling, giving rise to a ferromagnetic alignment tendency between sites on the same sublattice, but with unequal strength along the two diagonals d_1 and d_2. The notation $\langle i, j\rangle \in d_i$ is meant to signify a sum over nearest neighbors along only one diagonal. When $J_2 \neq J_2'$, $\mathcal{PT}$ symmetry is broken in the system, causing our model to exhibit altermagnetic properties. If we set $J_2 = J_2'$, the $\mathcal{PT}$ symmetry is reinstated, and our model reduces to an antiferromagnetic insulator with ferromagnetic intrasublattice exchange. The J_2/J_2' anisotropy is taken to be opposite for the A and B sublattices, which is evident from the terms with J_2 and J_2' in Eq. (2). Finally, $K < 0$ determines the easy-axis anisotropy strength along z, while ζ is the coupling strength to an external, time-dependent magnetic field $\boldsymbol{h}(r_i, t)$ which will drive the spin pumping and which can be nonhomogeneous in space. We shall assume the magnetic field takes the general form

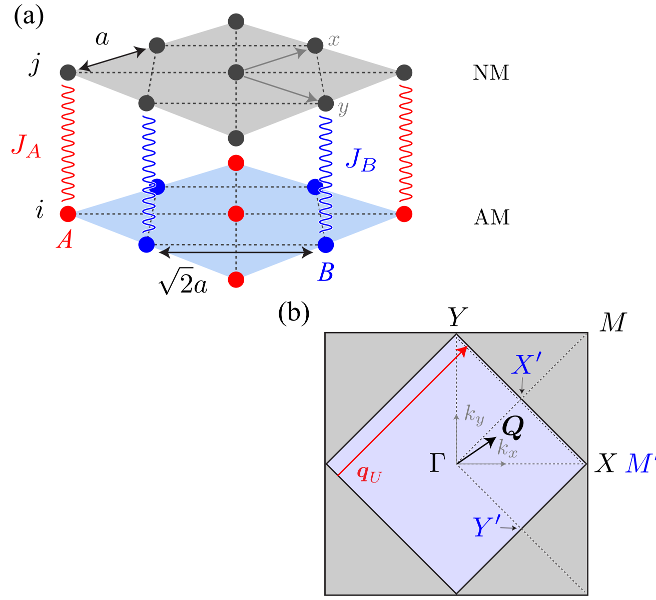

FIG. 2. (a) The altermagnetic (AM) and normal-metal (NM) layers are coupled by an interfacial, sublattice-dependent exchange coupling. Each site in the normal metal couples to the nearest neighbor in the altermagnetic layer with the sublattice-dependent J_A/J_B exchange coupling strength. (b) The NM Brillouin zone (BZ) is shown in gray, while the reduced BZ for momenta defined on the AM sublattices is shown in blue. $q_U = (\pi/a, \pi/a)$ is the umklapp vector. $\boldsymbol{Q}$ is the modulation vector which determines the spatial variation of the magnetic field.

$$\boldsymbol{h}(\boldsymbol{r}_i, t) = \cos(\boldsymbol{Q}\boldsymbol{r}_i)(h^x(t), h^y(t), 0), \qquad (3)$$

where the vector $\boldsymbol{Q}$ sets the spatial period of the magnetic field and we consider a field without a z component to simplify the calculations. By choosing $\boldsymbol{Q} = (0, 0)$, we obtain a spatially homogeneous magnetic field.

The normal-metal Hamiltonian is taken to be a simple tight-binding model with nearest-neighbor hopping, diagonalized with momentum-space operators,

$$H_{\mathrm{N}} = \sum_{\boldsymbol{k} \in \square, \sigma} \xi_{\boldsymbol{k}} c^\dagger_{\boldsymbol{k},\sigma} c_{\boldsymbol{k},\sigma}. \qquad (4)$$

The square lattice dispersion is given by $\xi_{\boldsymbol{k}} = -2t[\cos(k_x a) + \cos(k_y a)] - \mu$, where t is the hopping parameter and μ is the chemical potential. The $\boldsymbol{k}$ sum runs over the first Brillouin zone of the square lattice, denoted by $\square$.

The altermagnetic insulator and the normal metal are coupled by an interfacial exchange coupling (see Fig. 2),

$$H_{\mathrm{int}} = -2 \sum_{\langle i,j\rangle | i \in \mathrm{AM}, j \in \mathrm{NM}} J_i (c^\dagger_{j,\uparrow} c^\dagger_{j,\downarrow}) \boldsymbol{\sigma} \begin{pmatrix} c_{j,\uparrow} \\ c_{j,\downarrow} \end{pmatrix} \cdot \hat{\mathbf{S}}_i, \qquad (5)$$

where J_i for $i \in \{A, B\}$ is the sublattice-dependent interfacial exchange coupling strength and the sum runs over all sites on the interface. $\boldsymbol{\sigma}$ is the vector of the Pauli matrices. The nearest-neighbor notation $\langle i, j\rangle$ indicates that a given site i on the interface in the altermagnet couples only to the closest site j in the normal metal.

A. Diagonalizing the altermagnetic Hamiltonian

Introducing magnon operators for the two sublattices, A and B, the altermagnetic insulator Hamiltonian can, to second order in magnon operators, be written as $H_{\mathrm{AM}} = \sum_{\boldsymbol{q}\in\diamondsuit} \psi_{\boldsymbol{q}}^{\dagger} H_{\boldsymbol{q}} \psi_{\boldsymbol{q}}$, where $\psi_{\boldsymbol{q}} = (a_{\boldsymbol{q}}, b_{-\boldsymbol{q}}^{\dagger})^T$ and

$$H_{\boldsymbol{q}} = \begin{pmatrix} J^* + 2J_2\gamma_1 + 2J_2'\gamma_2 & 2J_1\gamma_3 \\ 2J_1\gamma_3 & J^* + 2J_2'\gamma_1 + 2J_2\gamma_2 \end{pmatrix}. \tag{6}$$

We have here defined $J^* = J_1 z - (J_2 + J_2')z/2 - 2K$ where $z = 4$ is the coordination number and the structure factors $\gamma_1 = \cos(q_x a + q_y a)$, $\gamma_2 = \cos(q_x a - q_y a)$, and $\gamma_3 = \cos q_x a + \cos q_y a$. The magnon momenta in the $\boldsymbol{q}$ sum runs over the reduced Brillouin zone (see Fig. 2), denoted by the diamond ($\diamondsuit$), corresponding to the Brillouin zone of one of the two sublattices. Introducing Bogoliubov quasiparticle operators $\alpha_{\boldsymbol{q}} = u_{\boldsymbol{q}} a_{\boldsymbol{q}} - v_{\boldsymbol{q}} b_{-\boldsymbol{q}}^{\dagger}$ and $\beta_{\boldsymbol{q}} = -v_{\boldsymbol{q}} a_{\boldsymbol{q}}^{\dagger} + u_{\boldsymbol{q}} b_{-\boldsymbol{q}}$, it follows that for

$$u_{\boldsymbol{q}} = \frac{1}{\sqrt{2}}\left(\frac{1}{\Delta} + 1\right), \quad v_{\boldsymbol{q}} = -\mathrm{sgn}(\gamma_3)\frac{1}{\sqrt{2}}\left(\frac{1}{\Delta} - 1\right), \tag{7}$$

and

$$\Delta = \sqrt{1 - \gamma_e^2}, \tag{8}$$

$$\gamma_e = \frac{2J_1\gamma_3}{4J_1 - 2K - (J_2 + J_2')(2 - \gamma_1 - \gamma_2)}, \tag{9}$$

the coefficients $u_{\boldsymbol{q}}$ and $v_{\boldsymbol{q}}$ diagonalize the Hamiltonian

$$H_{\mathrm{AM}} = \sum_{\boldsymbol{q}\in\diamondsuit} \begin{pmatrix} \alpha_{\boldsymbol{q}}^{\dagger} \\ \beta_{\boldsymbol{q}} \end{pmatrix} \begin{bmatrix} \omega_{\boldsymbol{q}}^{\alpha} & 0 \\ 0 & \omega_{\boldsymbol{q}}^{\beta} \end{bmatrix} \begin{pmatrix} \alpha_{\boldsymbol{q}} \\ \beta_{\boldsymbol{q}}^{\dagger} \end{pmatrix} + V, \tag{10}$$

with the quasiparticle eigenvalues

$$\omega_{\boldsymbol{q}}^{\alpha} = S\left[(J_2 - J_2')(\gamma_1 - \gamma_2) + \frac{2J_1\gamma_3\Delta}{\gamma_e}\right], \tag{11a}$$

$$\omega_{\boldsymbol{q}}^{\beta} = S\left[(J_2' - J_2)(\gamma_1 - \gamma_2) + \frac{2J_1\gamma_3\Delta}{\gamma_e}\right]. \tag{11b}$$

We note that due to the spatially anisotropic nature of H_{AM}, a momentum-dependent splitting arises between the two types of magnons in our system,

$$\Delta\omega = \left|\omega_{\boldsymbol{q}}^{\alpha} - \omega_{\boldsymbol{q}}^{\beta}\right| \tag{12}$$

$$= |2S(J_2 - J_2')(\gamma_1 - \gamma_2)|, \tag{13}$$

which is generally finite as long as $\boldsymbol{q}$ is not located on the high-symmetry paths Γ-M' in the reduced Brillouin zone (see Fig. 2).

The interaction term V in the diagonalized Hamiltonian stems from the coupling between $\hat{S}^x/\hat{S}^y$ and the external magnetic field and is given by

$$V = -\sum_{\pm} \lambda_{\pm\boldsymbol{Q}}[(\alpha_{\pm\boldsymbol{Q}} + \beta_{\pm\boldsymbol{Q}}^{\dagger})h^-(t) + (\alpha_{\pm\boldsymbol{Q}}^{\dagger} + \beta_{\pm\boldsymbol{Q}})h^+(t)], \tag{14}$$

where we have defined $\lambda_{\pm\boldsymbol{Q}} = \zeta\frac{\sqrt{N_A S}}{4}(u_{\pm\boldsymbol{Q}} + v_{\pm\boldsymbol{Q}})$ and $h^{\pm} = h_x \pm i h_y$ and $N_A = N/2$ is the number of lattice sites in the A sublattice. We shall assume throughout this paper that the numbers of lattice sites in the A and B sublattices are equal. Recall that $\boldsymbol{Q}$ characterizes the spatial inhomogeneity of the external magnetic field.

B. Interfacial exchange interaction

We now proceed by considering the interfacial exchange interaction between the altermagnetic insulator and the normal metal. Introducing magnon operators and performing a Bogoliubov transformation, Eq. (5) can be written as

$$H_{\mathrm{int}} = H_{\mathrm{int}}^{\parallel} + H_{\mathrm{int}}^{z}, \tag{15}$$

where we, to first order in magnon operators, have defined (see Appendix A for details)

$$H_{\mathrm{int}}^{\parallel} = -\sum_{\boldsymbol{q}\in\diamondsuit}\sum_{\boldsymbol{k}\in\square}\sum_{\kappa\in\{R,U\}}\sum_{\nu\in\{\alpha,\beta^{\dagger}\}} \times M_{\boldsymbol{q}}^{\nu\kappa}\nu_{\boldsymbol{q}} c_{\boldsymbol{k}^{\kappa},\downarrow}^{\dagger} c_{\boldsymbol{k}-\boldsymbol{q},\uparrow} + \mathrm{H.c.}, \tag{16}$$

$$H_{\mathrm{int}}^{z} = -\sqrt{2S}\sum_{\boldsymbol{k}\in\square}\sum_{\kappa\in\{R,U\}}(\overline{J}_A - \kappa\overline{J}_B) \times (c_{\boldsymbol{k}^{\kappa},\uparrow}^{\dagger} c_{\boldsymbol{k},\uparrow} - c_{\boldsymbol{k}^{\kappa},\downarrow}^{\dagger} c_{\boldsymbol{k},\downarrow}). \tag{17}$$

Here, we have defined $\kappa = R = 1$ and $\boldsymbol{k}^{\kappa} = \boldsymbol{k}^R = \boldsymbol{k}$ for the regular scattering process and $\kappa = U = -1$ and $\boldsymbol{k}^{\kappa} = \boldsymbol{k}^U = \boldsymbol{k} + \boldsymbol{q}_U$ for the umklapp process where the NM momenta $\boldsymbol{k}$ fall outside the reduced Brillouin zone of the altermagnetic insulator. $\boldsymbol{q}_U = (\pi/a, \pi/a)$ is the umklapp vector connecting the momenta $\boldsymbol{q}$ in the reduced Brillouin zone of the sublattices with the regular square lattice momenta $\boldsymbol{k}$. The coefficients $M_{\boldsymbol{q}}^{\nu\kappa}$ in Eq. (16) are defined as

$$M_{\boldsymbol{q}}^{\alpha\kappa} = \overline{J}_A u_{\boldsymbol{q}} + \kappa\overline{J}_B v_{\boldsymbol{q}}, \tag{18a}$$

$$M_{\boldsymbol{q}}^{\beta^{\dagger}\kappa} = \overline{J}_A v_{\boldsymbol{q}} + \kappa\overline{J}_B u_{\boldsymbol{q}}, \tag{18b}$$

and the modified exchange coefficients $\overline{J}_A$ and $\overline{J}_B$ are defined as

$$\overline{J}_A = 2\frac{\sqrt{2S}J_A N_A}{N_N\sqrt{N_A}}, \quad \overline{J}_B = 2\frac{\sqrt{2S}J_B N_B}{N_N\sqrt{N_B}}. \tag{19}$$

Here, N_N is the number of normal-metal sites at the interface, while N_A (N_B) is the number of sites on the A (B) sublattice at the interface. For the geometry studied in this paper, the number of sites at the interface is identical to the number of sites in general due to the two-dimensional geometry.

III. SPIN CURRENT

In order to obtain the spin current caused by the time-dependent external magnetic field in the altermagnet, we follow an approach similar to the one laid out by Kato *et al.* [19]. We consider the time dependence of the magnetization in the normal metal,

$$I_S = -\frac{d}{dt}\langle s^z\rangle = -i[H, s^z], \tag{20}$$

where all operators are in the Heisenberg picture and the normal-metal magnetization is given by

$$s^z = \frac{1}{2}\sum_{k\in\Box}(c^\dagger_{k,\uparrow}c_{k,\uparrow} - c^\dagger_{k,\downarrow}c_{k,\downarrow}). \tag{21}$$

As the fermionic number operators in the normal metal commute with the bosonic magnon operators of the altermagnetic insulator as well as with the fermionic number operators of H^z_{int}, $[H_{\text{AM}}, s^z] = [H^z_{\text{int}}, s^z] = 0$, and the only nonzero commutator to consider is the one with the in-plane interaction term $H^{\parallel}_{\text{int}}$. Writing out the time dependence and denoting the Heisenberg picture fermion and magnon operators via the superscript H, we get

$$[H^{\parallel}_{\text{int}}, s^z] = -\sum_{q\in\Diamond}\sum_{k\in\Box}\sum_{\kappa\in\{R,U\}}\sum_{\nu\in\{\alpha,\beta^\dagger\}} M^{\nu\kappa}_q \nu^H_q(t) c^{\dagger H}_{k^\kappa,\downarrow}(t) c^H_{k-q,\uparrow}(t) - \text{H.c.}$$

$$\Rightarrow I_S(t) = \text{Re}\left\{-2i\sum_{q\in\Diamond}\sum_{\kappa\in\{R,U\}}\sum_{\nu\in\{\alpha,\beta^\dagger\}}\left\langle M^{\nu\kappa}_q \nu^H_q(t) s^{\kappa-,H}_q(t)\right\rangle\right\} = 2\sum_{q\in\Diamond}\sum_{\kappa\in\{R,U\}}\sum_{\nu\in\{\alpha,\beta^\dagger\}}\text{Re}\{G^<_{q,\kappa,\nu}(t,t)\}, \tag{22}$$

where $I_S(t) \equiv \langle I_S\rangle$. Here, we have introduced the operator

$$s^{\kappa-,H}_q(t) := \sum_{k\in\Box} c^{\dagger H}_{k^\kappa,\downarrow}(t) c^H_{k-q,\uparrow}(t) \tag{23}$$

and defined the lesser Green's function

$$G^<_{q,\kappa,\nu}(t_1,t_2) = -i\left\langle M^{\nu\kappa}_q \nu^H_q(t_1) s^{\kappa-,H}_q(t_2)\right\rangle. \tag{24}$$

The average $\langle\cdots\rangle$ is taken in the ground state of the full time-dependent Hamiltonian. The terminology "lesser Green's function" is here used for this expectation value only because it will be evaluated by applying Langreth rules [20] to a corresponding contour-ordered expectation value for a choice of t_1 and t_2 that normally corresponds to a lesser Green's function.

In order to arrive at a final expression for the spin current I_S, we need to obtain an expression for the lesser Green's function in Eq. (24) at equal times $G^<_{q,\kappa,\nu}(t,t)$, including any relevant corrections due to the presence of a time-dependent magnetic field and the interfacial exchange interaction. This can be done by considering the related, contour-ordered Green's function

$$G_{\mathcal{C}}(t_1,t_2) = -i\left\langle T_{\mathcal{C}} M^{\nu\kappa}_q\left[\nu^H_q(t_1) s^{\kappa-,H}_q(t_2)\right]\right\rangle, \tag{25}$$

where $T_{\mathcal{C}}$ is the contour-ordering operator and the subscript $\mathcal{C}$ of the Green's function indicates that the time parameters t_1 and t_2 are defined on the Keldysh contour. We will explicitly choose t_1 to reside on the forward path and t_2 to reside on the backward path. For this choice of time parameters, it follows that the contour-ordered Green's function equals its lesser component,

$$G_{\mathcal{C}}(t_1,t_2) = G^<_{\mathcal{C}}(t_1,t_2) = -i\left\langle M^{\nu\kappa}_q \nu^H_q(t_1) s^{\kappa-,H}_q(t_2)\right\rangle, \tag{26}$$

which is precisely the expectation value we required to compute the spin current $I_S(t)$.

To proceed, we will compute the lesser component $G^<_{\mathcal{C}}$ in the interaction picture, considering the exchange interaction at the interface [Eqs. (16) and (17)] as a perturbation in the Keldysh formalism. The formal perturbation expansion is now given by [20,21]

$$G_{\mathcal{C}}(t_1,t_2) = -iM^{\nu\kappa}_q\left\langle T_{\mathcal{C}}\nu_q(t_1) s^{\kappa,-}_q(t_2) e^{-i\int_{\mathcal{C}} dt H_{\text{int}}(t)}\right\rangle_0. \tag{27}$$

The average $\langle\cdots\rangle_0$ is now taken in the absence of the interface interaction H_{int}, and the operators are defined in the interaction picture. We omit a superscript I on the operators for brevity of notation. In the following, we can ignore the contribution to H_{int} from H^z_{int} as the respective expectation values caused by this term will always be odd in magnon operators. We thus proceed by considering only the parallel term $H^{\parallel}_{\text{int}}$. Expanding Eq. (27) to first order in the perturbation and rewriting the contour-ordered Green's function as a Green's function over the regular time axis via the Langreth rules [21], we obtain the following lowest-order, nonvanishing contribution to the lesser Green's function in Eq. (22) (see Appendix B for details):

$$\begin{aligned} G^<_{q,\kappa,\nu}(t,t) = -i\int\frac{d\omega}{2\pi}\sum_{\kappa'\in\{R,U\}} M^{\nu\kappa}_q\left(M^{\nu\kappa'}_q\right)^* \\ \times\left[G^R_{\nu,q}(\omega)G^<_{s^+,\kappa\kappa',q}(\omega)\right. \\ \left. + G^<_{\nu,q}(\omega)G^A_{s^+,\kappa\kappa',q}(q,\omega)\right], \end{aligned} \tag{28}$$

where we have introduced the operator $s^{\kappa,+}_q = (s^{\kappa,-}_q)^\dagger$. If we let $\varphi \in \{\alpha, \beta^\dagger, s^+\}$, the corresponding lesser, retarded, and advanced Green's functions appearing in the equation above are given by

$$G^<_{\varphi,k}(t_1,t_2) = -i\langle\varphi^\dagger_k(t_2)\varphi_k(t_1)\rangle_0, \tag{29a}$$

$$G^R_{\varphi,k}(t_1,t_2) = -i\theta(t_1-t_2)\langle[\varphi_k(t_1),\varphi^\dagger_k(t_2)]\rangle_0, \tag{29b}$$

$$G^A_{\varphi,k}(t_1,t_2) = i\theta(t_2-t_1)\langle[\varphi_k(t_1),\varphi^\dagger_k(t_2)]\rangle_0, \tag{29c}$$

where the subscript 0 indicates an expectation value in the interaction picture, taken in the absence of time-dependent perturbations, thus making it equivalent to the Heisenberg picture without the interaction term V.

We now use the fact that the advanced and retarded Green's function components are related by $G^R_{\varphi,k}(\omega) = [G^A_{\varphi,k}(\omega)]^*$ as well as the definition of the distribution function,

$$f^\varphi(\omega,k) = \frac{G^<_{\varphi,k}(\omega)}{2i\text{Im}\{G^R_{\varphi,k}(\omega)\}}, \tag{30}$$

which, in equilibrium, is equal to the Bose-Einstein distribution $n_B(\omega,T)$ for bosons and also for the composite boson operator s^+ in the normal metal, which is bilinear in fermion operators. This can be proven using the Lehmann representation for the Green's function in equilibrium. Out of equilibrium, Eq. (30) also holds as the definition of the distribution function. This can be seen by noting that the particle density $n = \langle \varphi^\dagger(\boldsymbol{r}, t)\varphi(\boldsymbol{r}, t)\rangle$ for particle type φ is proportional to the lesser Green's function $G^<_\varphi$. At the same time, n should also be determined by an integral over the spectral weight times the distribution function for particle φ. Put differently, the number of particles should equal an integral over the available states times the probability that they are occupied. Since the denominator of Eq. (30) is precisely the spectral weight, moving it over to the left-hand side then shows how the particle density (determined by an integral over the lesser Green's function) is equal to an integral over the spectral weight times f^φ. Thus, f^φ is also the distribution function out of equilibrium.

IV. CORRECTIONS TO GREEN'S FUNCTIONS

In order to evaluate the spin current expression in Eq. (22) through the equal-time lesser component in Eq. (28), we will need Green's functions corresponding to the operators α, $\beta^\dagger$, and s^+. Below, we compute these quantities.

A. Spin pumping in the altermagnet

We consider first spin pumping in the altermagnet and the subsequent corrections to the α and $\beta^\dagger$ magnon Green's functions. We consider the interaction given by V [Eq. (14)] as a perturbation in the interaction picture. It can be shown that to second order in the interaction (see Appendix C for details), the retarded components of the Green's functions remain unaltered,

$$G^R_{\alpha,\boldsymbol{q}}(\omega) = \frac{1}{\omega - \omega^\alpha_{\boldsymbol{q}} + i\eta^\alpha}, \tag{31a}$$

$$G^R_{\beta^\dagger,\boldsymbol{q}}(\omega) = -G^A_{\beta,\boldsymbol{k}}(-\omega) = \frac{1}{\omega + \omega^\beta_{\boldsymbol{q}} + i\eta^\beta}, \tag{31b}$$

where η^ν can be considered the inverse lifetimes of the α and β magnons. The lesser component of the Green's functions picks up a second-order correction of the form

$$\Delta G^<_{\nu,\boldsymbol{q}}(\omega) = -4\pi i h_0^2 \delta(\omega - \Omega) \times \sum_\pm \lambda^2_{\pm\boldsymbol{Q}} \left|G^R_{\nu,\pm\boldsymbol{Q}}(\omega)\right|^2 \delta_{\boldsymbol{q},\pm\boldsymbol{Q}}, \tag{32}$$

where $\nu \in \{\alpha, \beta^\dagger\}$ and $\lambda_{\pm\boldsymbol{Q}}$ is defined under Eq. (14). Using Eq. (30), it then follows that the α and $\beta^\dagger$ magnon distribution functions pick up a correction due to the spin pumping, given to second order in the perturbation as

$$f^\nu(\omega, \boldsymbol{k}) = n_B(\omega, T) + \frac{2\pi h_0^2}{\eta^\nu}\delta(\omega - \Omega)\sum_\pm \lambda^2_{\pm\boldsymbol{Q}}\delta_{\boldsymbol{q},\pm\boldsymbol{Q}}. \tag{33}$$

B. Normal-metal spin susceptibility

We proceed by considering the retarded component of the spin susceptibility s^+ operator introduced in Eq. (23). Utilizing the fact that the normal-metal Hamiltonian is diagonal in momentum indices, it is straightforward to obtain the imaginary-time Matsubara Green's function $\overline{G}_{s^+,\boldsymbol{q}}(i\omega_n)$. The retarded susceptibility Green's function is then obtained by an analytical continuation

$$G^R_{s^+,\boldsymbol{q}}(\omega) = \overline{G}_{s^+,\boldsymbol{q}}(i\omega_n \to \omega + i\eta). \tag{34}$$

The retarded component is given by (see Appendix D for details)

$$G^R_{s^+,\kappa\kappa',\boldsymbol{q}}(\omega) = \delta_{\kappa,\kappa'}\sum_{\boldsymbol{k}\in\square}\frac{n_F(\xi_{\boldsymbol{k}-\boldsymbol{q}}, T) - n_F(\xi_{\boldsymbol{k}^\kappa}, T)}{\omega + \xi_{\boldsymbol{k}-\boldsymbol{q}} - \xi_{\boldsymbol{k}^\kappa} + i\eta^N}, \tag{35}$$

where n_F is the Fermi-Dirac distribution.

We now have all ingredients necessary to construct an explicit expression for the spin current. We take into account the appropriate corrections to the Green's functions due to spin pumping in the altermagnet as well as the perturbation caused by the interfacial exchange interaction. We also consider the relation between lesser components and the distribution function given in Eq. (30). It then follows that the spin current from Eq. (22) becomes

$$I_s(t) = -\sum_{\boldsymbol{q}\in\Diamond}\sum_{\kappa\in\{R,U\}}\sum_{\nu\in\{\alpha,\beta^\dagger\}}\mathrm{Re}\{G^<_{\boldsymbol{q},\kappa,\nu}(t,t)\} \tag{36}$$

$$= -4\pi h_0^2\int\frac{d\omega}{2\pi}\delta(\omega - \Omega)\sum_{\boldsymbol{q}\in\Diamond}\sum_{\kappa\in\{R,U\}}\sum_{\nu\in\{\alpha,\beta^\dagger\}}\left|M^{\nu\kappa}_{\boldsymbol{q}}\right|^2\frac{1}{\eta^\nu}\sum_\pm\lambda^2_{\pm\boldsymbol{Q}}\delta_{\boldsymbol{q},\pm\boldsymbol{Q}}\mathrm{Im}\{G^R_{\nu,\boldsymbol{q}}(\omega)\}\mathrm{Im}\{G^R_{s^+,\kappa,\boldsymbol{q}}(\omega)\} \tag{37}$$

$$= -2h_0^2\sum_{\kappa\in\{R,U\}}\sum_{\nu\in\{\alpha,\beta^\dagger\}}\sum_\pm\left|M^{\nu\kappa}_{\pm\boldsymbol{Q}}\right|^2\frac{\lambda^2_{\pm\boldsymbol{Q}}}{\eta^\nu}\mathrm{Im}\{G^R_{\nu,\pm\boldsymbol{Q}}(\Omega)\}\mathrm{Im}\{G^R_{s^+,\kappa,\pm\boldsymbol{Q}}(\Omega)\}, \tag{38}$$

and using the explicit forms of the Green's functions obtained above, we arrive at the final expression for the spin current,

$$I_s = \frac{NS\zeta^2h_0^2}{8}\sum_{\kappa\in\{R,U\}}\sum_\pm(u_{\pm\boldsymbol{Q}} + v_{\pm\boldsymbol{Q}})^2\left(\frac{\left|M^{\alpha\kappa}_{\pm\boldsymbol{Q}}\right|^2}{\left(\hbar\Omega - \omega^\alpha_{\pm\boldsymbol{Q}}\right)^2 + (\eta^\alpha)^2} + \frac{\left|M^{\beta^\dagger\kappa}_{\pm\boldsymbol{Q}}\right|^2}{\left(\hbar\Omega + \omega^\beta_{\pm\boldsymbol{Q}}\right)^2 + (\eta^\beta)^2}\right) \times \sum_{\boldsymbol{k}\in\square}\mathrm{Im}\left\{\frac{n_F(\xi_{\boldsymbol{k}-\boldsymbol{Q}}, T) - n_F(\xi_{\boldsymbol{k}^\kappa}, T)}{\hbar\Omega + \xi_{\boldsymbol{k}-\boldsymbol{Q}} - \xi_{\boldsymbol{k}^\kappa} + i\eta^N}\right\}. \tag{39}$$

Here, we have used the fact that the spin pumping in the altermagnet does not affect the normal-metal Hamiltonian, so that $f^{s+,\kappa}(\omega,\boldsymbol{k}) = n_B(\omega, T)$, where T is temperature.

V. RESULTS AND DISCUSSION

The final expression for the spin current lends itself to a simple interpretation. To first order in the external magnetic field, the field couples to magnons with wave vector $\pm\boldsymbol{Q}$ in the altermagnet. The result of this is that the spin current is peaked around the resonance frequencies $\hbar\Omega_R = \omega^{\alpha}_{\pm\boldsymbol{Q}}$ and $\hbar\Omega_R = -\omega^{\beta}_{\pm\boldsymbol{Q}}$. This means that the frequency at which the resonance takes place depends directly on the various exchange coefficients J_1, J_2, and J_2' in addition to the anisotropy K. The magnitude of the spin current response is affected by the imaginary part of the Lindhard function for the given frequency Ω. If we assume the NM broadening η^N is small, we can approximate the imaginary part of the Lindhard function as

$$\mathrm{Im}\{G^R_{s^+,\kappa,\pm\boldsymbol{Q}}(\Omega)\} \simeq \sum_{\boldsymbol{k}\in\Box}[n_F(\xi_{\boldsymbol{k}\mp\boldsymbol{Q}}) - n_F(\xi_{\boldsymbol{k}^\kappa})]\delta(\hbar\Omega + \xi_{\boldsymbol{k}\mp\boldsymbol{Q}} - \xi_{\boldsymbol{k}^\kappa}). \quad (40)$$

For a given choice of $\boldsymbol{Q}$ (the spatial modulation of the external field), this is, simply put, a sum over all physically available transitions in the NM separated by the energy $\hbar\Omega$. It is thus clear that depending on the frequency Ω, the magnitude of the spin current will be affected by the availability of electron states in the NM that have transitions between them due to the magnons reflecting off the interface and imparting energy, spin, and momentum to the normal metal. Specifically, the spin pumping field excites magnons in the altermagnet, and they cause spin-flip transitions in the normal metal which results in a net spin transfer across the interface. These spin-flip events must be such that Ω matches an allowed transition between electron states that conserves energy and momentum up to a reciprocal lattice vector in the altermagnet, the latter enabling umklapp scattering.

Before moving on, we briefly mention that we expect the presence of spin-flip scattering in the NM, for instance, mediated by magnetic impurities, to increase the magnitude of the spin pumping current. In the absence of spin-flip scattering, the spin pumping in the AM will lead to a spin accumulation in the NM which will counteract the spin current. If we instead have considerable spin-flip scattering in the NM, the accumulation will be prevented by spin conversion, causing the NM to behave as an effective spin sink. With this consideration in mind, we also expect that upon increasing the thickness of a NM with spin-flip scattering, the magnitude of the spin current will increase.

We now proceed by considering the spin current for different external field configurations.

A. Spin current for a homogeneous magnetic field

A homogeneous magnetic field is modeled by setting $\boldsymbol{Q} = (0.0, 0.0)$. Due to the form of the altermagnetic magnon correction caused by the external magnetic field, the spin current expression simplifies significantly in this case. The key observation is that in this case, the spin pumping correction to the magnon distribution functions $f^\nu(\omega,\boldsymbol{k})$ given in Eq. (33) is restricted to the spatially homogeneous mode $\boldsymbol{q} = (0.0, 0.0)$ through the Kronecker delta $\delta_{\boldsymbol{q},\pm\boldsymbol{Q}}$ from Eq. (32). This can intuitively be understood as a consequence of the external magnetic field $\boldsymbol{h}$ carrying no spatial dependence, thus causing a coupling between only the external field and the uniform magnon modes, to the chosen order of magnon operators. While a consideration of the uniform mode in spin pumping is not unusual in itself [5,22], the effect in this context is that the altermagnetic nature of the AM lattice disappears in the spin pumping contribution, leaving only the regular antiferromagnetic contribution.

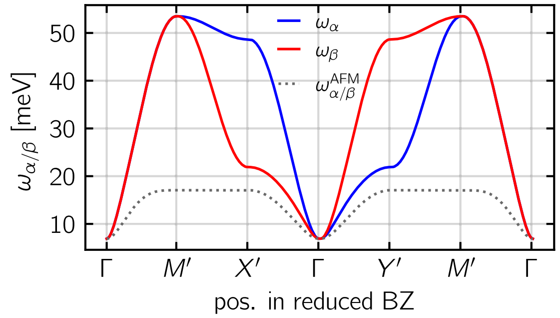

FIG. 3. Magnon spectra are shown for α (blue) and β (red) magnons in an altermagnet with $J_1 = 3.90, J_2 = -7.90, J_2' = -1.21$, and $K = -0.73$ meV. The dotted line shows the degenerate AFM magnon spectrum for the same J_1, but with $J_2 = J_2' = 0.0$. We observe that the three branches are all the same at the Γ point. Additionally, we note that Γ-M' is a special path in the BZ where the AM magnon spectrum is degenerate; in general, the splitting is nonzero away from Γ.

The disappearance of the altermagnetic character can be understood by considering the magnon dispersions in Eqs. (11a) and (11b) as well as the level splitting between the α and β magnons, given in Eq. (13). While for general momenta $\boldsymbol{q}$ they show a lifted degeneracy between the α and β branches, the splitting vanishes in the $\boldsymbol{q} \to \Gamma$ limit, as well as when $\boldsymbol{q}$ lies on the Γ-M' line (consider the magnon dispersion in Fig. 3). In particular at $\boldsymbol{q} = \Gamma$, the altermagnetic character of the system vanishes completely for the square lattice with coordination number $z = 4$ regardless of the values of J_2 and J_2'. When we then take into account that to first order in the perturbation, the external field with wave vector $\boldsymbol{Q}$ couples directly to magnons with wave vector $\boldsymbol{q} = \pm\boldsymbol{Q}$, the problem becomes obvious. In the present model and for a homogeneous field, the alter- and antiferromagnetic insulator is identical in terms of using the magnons in the magnetic insulator to drive a spin current.

B. Spin current for a nonhomogeneous magnetic field

Due to the above observations, we proceed directly to the consideration of a nonhomogeneous external field, comparing it to the homogeneous $\boldsymbol{Q} = (0.0, 0.0)$ antiferromagnetic (AFM) spin current. We use a NM hopping parameter $t = 500$ meV, $J_1 = 3.90$ meV, $J_2 = -7.90$ meV, $J_2' = -1.21$ meV, and an easy-axis anisotropy $K = -0.73$ meV. The particular exchange coefficients are obtained through *ab initio* methods and were originally presented in Ref. [14].

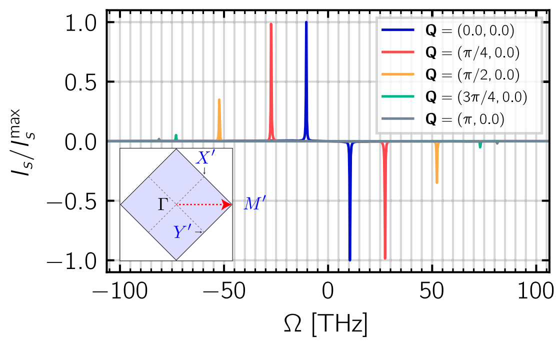

FIG. 4. Altermagnet/normal-metal spin current I_s as a function of field frequency Ω, normalized on the maximum AFM spin current with a uniform magnetic field using $J_1 = 3.90$, $J_2 = -7.90$, $J_2' = -1.21$, and $K = -0.73$ meV. The $\boldsymbol{Q} = (0.0, 0.0)$ spin current is essentially the AFM-NM spin current as AM character vanishes at the Γ point. We let $\boldsymbol{Q}$ move along Γ-M', indicated by the red arrow in the inset, which is the X point in the NM Brillouin zone. Along this path, the AM magnon spectrum is degenerate. This means that the resonance frequency Ω_R changes with $\boldsymbol{Q}$ but we have the same resonance frequencies for positive and negative Ω. As $\mathrm{Im}\{G_{s^+}(\Omega)\} = -\mathrm{Im}\{G_{s^+}(-\Omega)\}$, the positive and negative frequency peaks have the same magnitude, but with opposite signs.

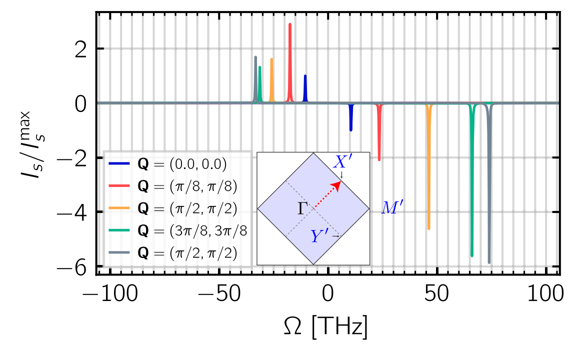

FIG. 5. Altermagnet/normal-metal spin current I_s as a function of field frequency Ω, normalized on the maximum AFM spin current with a uniform magnetic field using $J_1 = 3.90$, $J_2 = -7.90$, $J_2' = -1.21$, and $K = -0.73$ meV. We let $\boldsymbol{Q}$ move along Γ-X', indicated by the red arrow in the inset, which is halfway to the NM BZ M point. We observe that a consequence of the splitting between α and β magnons is that the resonance frequencies at which the spin current peaks are located are no longer symmetric around $\Omega = 0$. We also observe that the magnitudes of the positive and negative frequency peaks are now different as $\mathrm{Im}\{G_{s^+}(\Omega)\}$ now gives a different weight for the positive and negative resonance frequencies.

While the results in the following depend on these coefficients, our findings are general and are expected to be generally present for systems with the appropriate altermagnetic symmetries. Finally, the chemical potential in the NM is set to $\mu = 0.0$, the half-filled case. We set the magnon broadening to $\eta^{\alpha/\beta} = 0.1$ meV and the NM broadening, modeling, e.g., inelastic electron-phonon or electron-electron interactions, to $\eta^N = 1$ meV and use a reciprocal temperature $1/k_B T = 0.1$ meV^{-1}, corresponding to a temperature of around 116 K.

We begin by considering an external field whose spatial modulation is oriented along the Γ-M' line, as depicted in Fig. 4. Along this high-symmetry path, the magnon branches are degenerate. We observe that as $\boldsymbol{Q}$ increases in magnitude, the resonance frequencies Ω_R increase as well. Considering the magnon dispersion in Fig. 3, this is as expected because we are coupling higher-energy magnons with increasing $\boldsymbol{Q}$. The resonance peaks are symmetric around $\Omega = 0$ and equal in magnitude for $\Omega = \pm\Omega_R$, which is as expected since $\mathrm{Im}\{G_{s^+}(\Omega)\} = -\mathrm{Im}\{G_{s^+}(-\Omega)\}$. This behavior is qualitatively similar to that of spin pumping in an AFM/NM bilayer. As $\boldsymbol{Q}$ moves away from the Γ point, the energy of the magnons which couple to the field changes with a subsequent shift in the resonance frequency Ω_{R}. As the magnon branches are degenerate along this path in the AM Brillouin zone, the resonance frequencies Ω_{R} are symmetric around zero. Recall that the positive and negative resonance frequencies are set by $\omega^{\alpha}_{\pm\boldsymbol{Q}}$ and $-\omega^{\beta}_{\pm\boldsymbol{Q}}$, respectively, the magnitudes of which are the same for a degenerate dispersion. For an antiferromagnet, this behavior is expected for any $\boldsymbol{Q}$ in the Brillouin zone (BZ) due to the degenerate magnon branches. This suggests that for $\boldsymbol{Q}$ lying on the Γ-M' path in the AM BZ, the spin pumping behavior is qualitatively similar to that of an antiferromagnet, but with resonance frequencies and magnitudes dependent on the various exchange coefficients as well as the anisotropy. The effect of $\boldsymbol{Q}$ on the magnitude of the spin current is discussed at the end of this section.

The similarities between AFM and AM spin pumping vanish when we consider $\boldsymbol{Q}$ away from the Γ-M' line of magnon degeneracy, i.e., the most probable case because the degeneracy is present only exactly at the Γ-M' line. Then, we couple to α and β magnons with different energies $\omega^{\alpha} \neq \omega^{\beta}$. Taking into consideration that the α and β magnons give rise to the positive and negative resonances, respectively, the breaking of the magnon degeneracy implies the emergence of an asymmetry between the positive and negative resonance frequencies. This is also clear from Fig. 5, where we consider $\boldsymbol{Q}$ on the Γ-X' line in the reduced BZ. Along this path, α magnons have higher energies than the β magnons, something which manifests in the higher magnitudes of the positive resonance frequencies as opposed to the negative ones. We emphasize that this asymmetry is not a fine-tuning effect, but rather the expected behavior for an arbitrary spatial modulation $\boldsymbol{Q}$. It is only when the modulation matches the high-symmetry paths of magnon degeneracy that we regain the frequency-symmetric characteristics associated with the antiferromagnet. We thus expect that this should be possible to verify experimentally. As mentioned above, the magnitude of the spin current is determined in part by the Lindhard function, i.e., by the presence of available transitions in the NM. As the positive and negative resonances now are different, their magnitudes, given in part by the susceptibility Lindhard function, are also, in general, different, giving rise to a highly asymmetrical spin current behavior which is asymmetric in both resonance frequency and magnitude.

We finally mention that the magnitudes of the spin currents depicted in Figs. 4 and 5, normalized on the $\boldsymbol{Q} = (0.0, 0.0)$ AFM spin current, are highly dependent on the specific parameters of the system. In general, the energy of the AM magnons is on the order of 1–10 meV, which, as is well known, gives rise to the desirable terahertz frequency response. The energy of the NM electrons, reflected through the hopping parameter t, is generally on the order of 1 eV. This mismatch of energy scales will generally decrease the number of available transitions in the NM, as shown in Eq. (40). This can give rise to large observed variation in spin current magnitudes due to the interplay between the resonance frequency Ω_R set by the AM magnon dispersion and the particular number of available transitions at the specific value of $\boldsymbol{Q}$. We nevertheless draw the conclusion that for $\boldsymbol{Q}$ close to the Γ point, the results indicate that it is possible to obtain a spin current which is comparable in magnitude to a regular antiferromagnet but has novel features such as the nonsymmetric resonance frequencies and subsequent pumping modified magnitudes. We expect that this also holds when replacing the normal metal with a superconductor, as was recently studied [23] in the antiferromagnetic case. Spin pumping from a ferromagnetic insulator into an altermagnetic metal was studied in Ref. [24].

VI. SUMMARY

We computed spin pumping from an altermagnetic insulator into a normal metal using a nonequilibrium Keldysh Green's function perturbation technique. The altermagnetic model introduced in Ref. [14], consisting of two intercalated square sublattices with a spin order that breaks $\mathcal{PT}$ symmetry, was used. Our calculations showed that for a homogeneous magnetic field, the spin current pumped from the altermagnet is the same as the spin current pumped from a conventional square lattice antiferromagnet with Néel order. When the magnetic field becomes spatially dependent, however, the spin pumping characteristics become dependent on the altermagnetic crystal orientation. Along the high-symmetry paths of magnon degeneracy in the altermagnet, the spin current behavior retains its antiferromagnetic character, but for general modulation vectors $\boldsymbol{Q}$ away from these paths, the spin current response of the altermagnet is different from that of an antiferromagnet. In particular, the resonance frequencies become nonsymmetric in frequency due to the broken magnon degeneracy. These results demonstrate that while the spin order in an altermagnet can give rise to terahertz spin pumping like for a regular antiferromagnet, the pumping behavior can be qualitatively different depending on the relation between the spatial modulation of the magnetic field and the crystal orientation.

ACKNOWLEDGMENTS

We thank B. Brekke and C. Sun for helpful discussions. This work was supported by the Research Council of Norway through Grant No. 323766 and its Centres of Excellence funding scheme through Grant No. 262633 "QuSpin." Support from Sigma2, the National Infrastructure for High Performance Computing and Data Storage in Norway, Project No. NN9577K, is acknowledged.

APPENDIX A: INTERFACIAL EXCHANGE INTERACTION

We consider the interaction term in more detail, considering the geometry depicted in Fig. 1:

$$\begin{aligned} H_{\mathrm{int}} &= -2 \sum_{\langle i,j\rangle | i\in \mathrm{AF}, j\in \mathrm{NM}} J_i (c_{j,\uparrow}^\dagger c_{j,\downarrow}^\dagger) \boldsymbol{\sigma} \begin{pmatrix} c_{j,\uparrow} \\ c_{j,\downarrow} \end{pmatrix} \cdot \hat{\boldsymbol{S}}_i \\ &= -2 \sum_{\substack{\langle i,j\rangle \\ i\in A, j\in \mathrm{NM}}} J_A [S_{iA}^- c_{j,\uparrow}^\dagger c_{j,\downarrow} + S_{iA}^+ c_{j,\downarrow}^\dagger c_{j,\uparrow}] + S_{iA}^z (c_{j,\uparrow}^\dagger c_{j,\uparrow} - c_{j,\downarrow}^\dagger c_{j,\downarrow}) \\ &\quad - 2 \sum_{\substack{\langle i,j\rangle \\ i\in B, j\in \mathrm{NM}}} J_B [S_{iB}^- c_{j,\uparrow}^\dagger c_{j,\downarrow} + S_{iB}^+ c_{j,\downarrow}^\dagger c_{j,\uparrow}] + S_{iB}^z (c_{j,\uparrow}^\dagger c_{j,\uparrow} - c_{j,\downarrow}^\dagger c_{j,\downarrow}) \\ &= -2 \left(\sum_{\substack{\langle i,j\rangle \\ i\in A}} J_A S_{iA}^+ c_{j,\downarrow}^\dagger c_{j,\uparrow} + \mathrm{H.c.} + \sum_{\substack{\langle i,j\rangle \\ i\in B}} J_B S_{iB}^+ c_{j,\downarrow}^\dagger c_{j,\uparrow} + \mathrm{H.c.} \right) + H_{\mathrm{int}}^z, \end{aligned} \tag{A1}$$

where

$$H_{\mathrm{int}}^z = -2 \sum_{\substack{\langle i,j\rangle \\ i\in A}} S_{iA}^z (c_{j,\uparrow}^\dagger c_{j,\uparrow} - c_{j,\downarrow}^\dagger c_{j,\downarrow}) - 2 \sum_{\substack{\langle i,j\rangle \\ i\in B}} S_{iB}^z (c_{j,\uparrow}^\dagger c_{j,\uparrow} - c_{j,\downarrow}^\dagger c_{j,\downarrow}). \tag{A2}$$

Leaving H_{int}^z aside for now, we shall denote the rest of the terms as $H_{\mathrm{int}}^{\parallel}$. The term in $H_{\mathrm{int}}^{\parallel}$ running over the A sublattice becomes

$$\begin{aligned} -2 \sum_{\substack{\langle i,j\rangle \\ i\in A}} J_A S_{iA}^+ c_{j,\downarrow}^\dagger c_{j,\uparrow} &= -2 \frac{\sqrt{2S} J_A}{N_N \sqrt{N_A}} \sum_{i\in A} \sum_{\boldsymbol{q}\in\Diamond} \sum_{\boldsymbol{k}_1,\boldsymbol{k}_2\in\square} a_{\boldsymbol{q}} c_{\boldsymbol{k}_1,\downarrow}^\dagger c_{\boldsymbol{k}_2,\uparrow} e^{i\boldsymbol{q}\cdot\boldsymbol{r}_i} e^{i(\boldsymbol{k}_2-\boldsymbol{k}_1)\cdot(\boldsymbol{r}_i + a\hat{\boldsymbol{z}})} \\ &= -\frac{\bar{J}_A}{N_A} \sum_{i\in A} \sum_{\boldsymbol{q}\in\Diamond} \sum_{\boldsymbol{k}_1,\boldsymbol{k}_2\in\square} a_{\boldsymbol{q}} c_{\boldsymbol{k}_1,\downarrow}^\dagger c_{\boldsymbol{k}_2,\uparrow} e^{i(\boldsymbol{k}_2-\boldsymbol{k}_1+\boldsymbol{q})\cdot\boldsymbol{r}_i} e^{ia(\boldsymbol{k}_2-\boldsymbol{k}_1)\cdot\hat{\boldsymbol{z}}}, \end{aligned} \tag{A3}$$

where $\bar{J}_A = 2\sqrt{2S} J_A N_A / (N_N \sqrt{N_A})$ and we have assumed the spacing between the altermagnetic and normal-metal layer is $a\hat{\boldsymbol{z}}$, where a is the lattice parameter. The last exponential factor becomes unity as $\boldsymbol{k}_1$ and $\boldsymbol{k}_2$ run in the xy plane. In order to connect the Brillouin zone of the normal metal to the reduced Brillouin zone of the altermagnetic lattice, we rewrite the sum over the regular Brillouin zone as $\sum_{\boldsymbol{k}\in\square} f(\boldsymbol{k}) = \sum_{\boldsymbol{k}\in\lozenge}[f(\boldsymbol{k}) + f(\boldsymbol{k}+\boldsymbol{Q})]$, where $Q = \pi/a\hat{\boldsymbol{x}} + \pi/a\hat{\boldsymbol{y}}$ is the vector connecting the two. It then follows that

$$\begin{aligned}
&-\frac{\bar{J}_A}{N_A}\sum_{i\in A}\sum_{\boldsymbol{q}\in\lozenge}\sum_{\boldsymbol{k_1},\boldsymbol{k_2}\in\square} a_{\boldsymbol{q}} c^\dagger_{\boldsymbol{k}_1,\downarrow} c_{\boldsymbol{k}_2,\uparrow} e^{i(\boldsymbol{k}_2-\boldsymbol{k}_1+\boldsymbol{q})\cdot\boldsymbol{r}_i}\\
&= -\frac{\bar{J}_A}{N_A}\sum_{i\in A}\sum_{\boldsymbol{q}\in\lozenge}\sum_{\boldsymbol{k_1},\boldsymbol{k_2}\in\lozenge} a_{\boldsymbol{q}} e^{i\boldsymbol{q}\cdot\boldsymbol{r}_i}\big[\big(c^\dagger_{\boldsymbol{k}_1,\downarrow}e^{-i\boldsymbol{k}_1\cdot\boldsymbol{r}_i} + c^\dagger_{\boldsymbol{k}_1^U,\downarrow}e^{-i\boldsymbol{k}_1^U\cdot\boldsymbol{r}_i}\big)\big(c_{\boldsymbol{k}_2,\uparrow}e^{i\boldsymbol{k}_2\cdot\boldsymbol{r}_i} + c_{\boldsymbol{k}^U,\downarrow}e^{i\boldsymbol{k}_2^U\cdot\boldsymbol{r}_i}\big)\big]\\
&= -\bar{J}_A\sum_{\boldsymbol{q}\in\lozenge}\sum_{\boldsymbol{k}\in\square} a_{\boldsymbol{q}} c^\dagger_{\boldsymbol{k},\downarrow} c_{\boldsymbol{k}-\boldsymbol{q},\uparrow} + \kappa a_{\boldsymbol{q}} c^\dagger_{\boldsymbol{k}^U,\downarrow} c_{\boldsymbol{k}-\boldsymbol{q},\uparrow},
\end{aligned} \tag{A4}$$

where we have defined the umklapp momentum $\boldsymbol{k}^U = \boldsymbol{k} + \boldsymbol{Q}$ and $\kappa = 1$ for $\boldsymbol{r}_i \in A$ and $\kappa = -1$ for $\boldsymbol{r}_i \in B$, arising from the factor $e^{i\boldsymbol{Q}\cdot\boldsymbol{r}_i}$ in the cross terms. Performing the analogous calculation for the B sublattice gives the final interaction term,

$$H^{\parallel}_{\text{int}} = -\sum_{\boldsymbol{q}\in\lozenge}\sum_{\boldsymbol{k}\in\square}\big(M^{\alpha R}_{\boldsymbol{q}}\alpha_{\boldsymbol{q}} + M^{\beta^\dagger R}_{\boldsymbol{q}}\beta^\dagger_{\boldsymbol{q}}\big)c^\dagger_{\boldsymbol{k},\downarrow}c_{\boldsymbol{k}-\boldsymbol{q},\uparrow} + \big(M^{\alpha U}_{\boldsymbol{q}}\alpha_{\boldsymbol{q}} + M^{\beta^\dagger U}_{\boldsymbol{q}}\beta^\dagger_{\boldsymbol{q}}\big)c^\dagger_{\boldsymbol{k}^U,\downarrow}c_{\boldsymbol{k}-\boldsymbol{q},\uparrow} + \text{H.c.}, \tag{A5}$$

where we have defined

$$M^{\alpha\kappa}_{\boldsymbol{q}} = (\bar{J}_A u_{\boldsymbol{q}} + \kappa\bar{J}_B v_{\boldsymbol{q}}), \quad M^{\beta^\dagger\kappa}_{\boldsymbol{q}} = (\bar{J}_A v_{\boldsymbol{q}} + \kappa\bar{J}_B u_{\boldsymbol{q}}), \tag{A6}$$

where $\kappa = 1$ for the regular scattering process (R) and $\kappa = -1$ for the umklapp process (U). Rewriting this finally as a sum over the operators $\{\alpha_{\boldsymbol{q}}, \beta^\dagger_{\boldsymbol{q}}\}$, we obtain

$$H^{\parallel}_{\text{int}} = -\sum_{\boldsymbol{q}\in\lozenge}\sum_{\boldsymbol{k}\in\square}\sum_{\kappa\in\{R,U\}}\sum_{\nu\in\{\alpha,\beta^\dagger\}} M^{\nu\kappa}_{\boldsymbol{q}}\nu_{\boldsymbol{q}}c^\dagger_{\boldsymbol{k}^\kappa,\downarrow}c_{\boldsymbol{k}-\boldsymbol{q},\uparrow} + \text{H.c.} \tag{A7}$$

We now consider H^z_{int}. To first order in the magnon operators, the term becomes

$$\begin{aligned}
H^z_{\text{int}} &= -2\sum_{\substack{\langle i,j\rangle\\ i\in A}} J_A S(c^\dagger_{j,\uparrow}c_{j,\uparrow} - c^\dagger_{j,\downarrow}c_{j,\downarrow}) - 2\sum_{\substack{\langle i,j\rangle\\ i\in B}} J_B(-S)(c^\dagger_{j,\uparrow}c_{j,\uparrow} - c^\dagger_{j,\downarrow}c_{j,\downarrow})\\
&= -\frac{2J_AS}{N_N\sqrt{N_A}}\sum_{i\in A}\sum_{\boldsymbol{k}_1,\boldsymbol{k}_2\in\square}(c^\dagger_{\boldsymbol{k}_1,\uparrow}c_{\boldsymbol{k}_2,\uparrow} - c^\dagger_{\boldsymbol{k}_1,\downarrow}c_{\boldsymbol{k}_2,\downarrow})e^{-i(\boldsymbol{k}_1-\boldsymbol{k}_2)\cdot(\boldsymbol{r}_i+a\hat{z})} - \frac{2J_BS}{N_N\sqrt{N_B}}\sum_{i\in B}\\
&\quad\times\sum_{\boldsymbol{k}_1,\boldsymbol{k}_2\in\square}(c^\dagger_{\boldsymbol{k}_1,\uparrow}c_{\boldsymbol{k}_2,\uparrow} - c^\dagger_{\boldsymbol{k}_1,\downarrow}c_{\boldsymbol{k}_2,\downarrow})e^{-i(\boldsymbol{k}_1-\boldsymbol{k}_2)\cdot(\boldsymbol{r}_i+a\hat{z})}\\
&= -\sqrt{2S}\sum_{\boldsymbol{k}\in\square}(\bar{J}_A - \bar{J}_B)(c^\dagger_{\boldsymbol{k},\uparrow}c_{\boldsymbol{k},\uparrow} - c^\dagger_{\boldsymbol{k},\downarrow}c_{\boldsymbol{k},\downarrow}) + (\bar{J}_A + \bar{J}_B)(c^\dagger_{\boldsymbol{k}+\boldsymbol{Q},\uparrow}c_{\boldsymbol{k},\uparrow} - c^\dagger_{\boldsymbol{k}+\boldsymbol{Q},\downarrow}c_{\boldsymbol{k},\downarrow})\\
&= -\sqrt{2S}\sum_{\boldsymbol{k}\in\square}\sum_{\kappa\in\{R,U\}}(\bar{J}_A - \kappa\bar{J}_B)(c^\dagger_{\boldsymbol{k}^\kappa,\uparrow}c_{\boldsymbol{k},\uparrow} - c^\dagger_{\boldsymbol{k}^\kappa,\downarrow}c_{\boldsymbol{k},\downarrow}).
\end{aligned} \tag{A8}$$

APPENDIX B: SPIN CURRENT DERIVATION

We treat the spin current lesser Green's function in the interaction picture with the exchange interaction at the interface as a perturbation in the Keldysh formalism. The starting point is the lesser component of the contour-ordered Green's function for a given set of parameters ν, $\boldsymbol{q}$, and κ (these indices are omitted in the following for brevity of notation),

$$G_{\mathcal{C}}(t_1,t_2) = G^<_{\mathcal{C}}(t_1,t_2) = -i\big\langle M^{\nu\kappa}_{\boldsymbol{q}}\nu^H_{\boldsymbol{q}}(t_1)s^{\kappa,-,H}_{\boldsymbol{q}}(t_2)\big\rangle. \tag{B1}$$

We now go to the interaction picture where we treat $H^{\parallel}_{\text{int}}$ as a perturbation. It then follows that the full Green's function may be written as

$$G_{\mathcal{C}}(t_1,t_2) = -iM^{\nu\kappa}_{\boldsymbol{q}}\big\langle T_{\mathcal{C}}\nu_{\boldsymbol{q}}(t_1)s^{\kappa,-}_{\boldsymbol{q}}(t_2)e^{-i\int_{\mathcal{C}}dtH^{\parallel}_{\text{int}}(t)}\big\rangle_0, \tag{B2}$$

where $\mathcal{T}_{\mathcal{C}}$ is the contour-ordering operator placing operators with time arguments later on the contour to the left and earlier on the right.

Expanding the exponential to first order in $H_{\text{int}}^{\parallel}$, we obtain

$$G_{\mathcal{C}}^{<}(t_1,t_2) - G_{\mathcal{C}}^{<,0}(t_1,t_2) \simeq -\left\langle \mathcal{T}_{\mathcal{C}} \int_{\mathcal{C}} dt \sum_{\boldsymbol{q}'\in\Diamond} \sum_{\kappa'\in\{R,U\}} \sum_{\nu'\in\{\alpha,\beta^\dagger\}} M_{\boldsymbol{q}}^{\nu\kappa} \left(M_{\boldsymbol{q}'}^{\nu'\kappa'}\right)^* \nu_{\boldsymbol{q}}(t_1) s_{\boldsymbol{q}}^{\kappa,-}(t_2) \nu'^{\dagger}_{\boldsymbol{q}'}(t) s_{\boldsymbol{q}'}^{\kappa',+}(t) \right\rangle_0 + \mathcal{O}\left(H_{\text{int}}^2\right) \tag{B3}$$

$$= -\sum_{\boldsymbol{q}'\in\Diamond} \sum_{\kappa'\in\{R,U\}} \sum_{\nu'\in\{\alpha,\beta^\dagger\}} M_{\boldsymbol{q}}^{\nu\kappa} \left(M_{\boldsymbol{q}'}^{\nu'\kappa'}\right)^* \int_{\mathcal{C}} dt \langle T_{\mathcal{C}} \nu_{\boldsymbol{q}}(t_1) \nu'^{\dagger}_{\boldsymbol{q}'}(t)\rangle_0 \left\langle T_{\mathcal{C}} s_{\boldsymbol{q}}^{\kappa,-}(t_2) s_{\boldsymbol{q}'}^{\kappa',+}(t)\right\rangle_0 \tag{B4}$$

$$= \sum_{\kappa'\in\{R,U\}} M_{\boldsymbol{q}}^{\nu\kappa} \left(M_{\boldsymbol{q}}^{\nu\kappa'}\right)^* \left[G_\nu(\boldsymbol{q}) \bullet\ G_{s^+}^{\kappa\kappa'}(\boldsymbol{q})\right](t_1,t_2), \tag{B5}$$

where $s_{\boldsymbol{q}}^{\kappa,+} = (s_{\boldsymbol{q}}^{\kappa,-})^\dagger$, we have defined the Green's functions

$$G_\nu(\boldsymbol{q};t,t') = -i\langle T_{\mathcal{C}} \nu_{\boldsymbol{q}}(t) \nu'^{\dagger}_{\boldsymbol{q}}(t')\rangle_0, \tag{B6}$$

$$G_{s^+}^{\kappa\kappa'}(\boldsymbol{q};t,t') = -i\left\langle T_{\mathcal{C}} s_{\boldsymbol{q}}^{\kappa',+}(t) s_{\boldsymbol{q}}^{\kappa,-}(t')\right\rangle_0, \tag{B7}$$

and the bullet product $\bullet$ denotes integration of the internal time parameter t along the contour and is defined by

$$(A\bullet B)(t_1,t_2) = \int_{\mathcal{C}} dt A(t_1,t) B(t,t_2). \tag{B8}$$

Note that in Eq. (B5), we have used the fact that the Hamiltonian is diagonal in magnon operators α and $\beta^\dagger$ as well as magnon momentum $\boldsymbol{q}$ to eliminate two of the summations. As indicated by the superscript $<$, we consider the lesser component of the contour-ordered Green's function $G_{\mathcal{C}}(t_1,t_2)$. We proceed by utilizing the Langreth rules [21]. If

$$C(t_1,t_2) = (A\bullet B)(t_1,t_2), \tag{B9a}$$

$$D(t_1,t_2) = (A\bullet B\bullet C)(t_1,t_2), \tag{B9b}$$

the advanced, retarded, and lesser components of C and D satisfy

$$C^< = A^R\circ B^< + A^<\circ B^A, \tag{B10a}$$

$$C^{R/A} = A^{R/A}\circ B^{R/A}, \tag{B10b}$$

$$D^< = A^R\circ B^R\circ C^< + A^R\circ B^<\circ C^A + A^<\circ B^A\circ C^A, \tag{B10c}$$

$$D^{R/A} = A^{R/A}\circ B^{R/A}\circ C^{R/A}, \tag{B10d}$$

where we have defined the circle product

$$(A\circ B)(t_1,t_2) = \int_{-\infty}^{\infty} dt A(t_1,t) B(t,t_2). \tag{B11}$$

From this, it then follows that

$$G_{\mathcal{C}}^<(t_1,t_2) = \sum_{\kappa'\in\{R,U\}} M_{\boldsymbol{q}}^{\nu\kappa}\left(M_{\boldsymbol{q}}^{\nu\kappa'}\right)^*\left[G_\nu^R(\boldsymbol{q})\circ G_{s^+}^{\kappa\kappa',<}(\boldsymbol{q}) + G_\nu^<(\boldsymbol{q})\circ G_{s^+}^{\kappa\kappa',A}(\boldsymbol{q})\right](t_1,t_2). \tag{B12}$$

The time integration reduces to a regular convolution integral as $G_\psi^R(t_1,t_2)$ and $G_\psi^<(t_1,t_2)$ depend only on the relative time t_1-t_2. The lesser component then becomes, upon a Fourier transformation of the Green's functions, a simple product. Since we need $G_{\mathcal{C}}^<$ at equal times to compute the spin current, we now set $t_1=t_2=t$. Considering then, for example, the first term of $G_{\mathcal{C}}^<$, it follows, omitting momentum indices for brevity, that

$$\begin{aligned} G_\nu^R\circ G_{s^+}^{\kappa\kappa',<}(t,t) &= \int_{-\infty}^{\infty} dt' G_\nu^R(t,t') G_{s^+}^{\kappa\kappa',<}(t',t) \\ &= \int_{-\infty}^{\infty} dt' \int \frac{d\omega}{2\pi}\frac{d\omega'}{2\pi} e^{i\omega(t-t')} e^{i\omega'(t'-t)} G_\nu^R(\omega) G_{s^+}^{\kappa\kappa',<}(\omega') \\ &= \int \frac{d\omega}{2\pi} G_\nu^R(\omega) G_{s^+}^{\kappa\kappa',<}(\omega). \end{aligned} \tag{B13}$$

The final expression for the correction to the lesser component of $G_{\boldsymbol{q},\kappa,\nu}^<(t,t)$ from Eq. (22), found by using the contour-ordered Green's function $G_{\mathcal{C}}^<$, is then given by

$$\begin{aligned} G_{\boldsymbol{q},\kappa,\nu}^<(t,t) - G_{\boldsymbol{q},\kappa,\nu}^{<,0}(t,t) &= \int \frac{d\omega}{2\pi} \sum_{\kappa'\in\{R,U\}} M_{\boldsymbol{q}}^{\nu\kappa}\left(M_{\boldsymbol{q}}^{\nu\kappa'}\right)^*\left[G_\nu^R(\boldsymbol{q},\omega) G_{s^+}^{\kappa\kappa',<}(\boldsymbol{q},\omega) \right. \\ &\quad \left. + G_\nu^<(\boldsymbol{q},\omega) G_{s^+}^{\kappa\kappa',A}(\boldsymbol{q},\omega)\right]. \end{aligned} \tag{B14}$$

APPENDIX C: SPIN PUMPING IN THE ALTERMAGNET

We now introduce an explicit time dependence $h^\pm(t) = h_0 e^{\mp i\Omega t}$, where Ω is the field frequency. We now want to treat Eq. (14) as a perturbation,

$$V = -\sum_{\pm} \lambda_{\pm\boldsymbol{Q}}[(\alpha_{\pm\boldsymbol{Q}} + \beta^\dagger_{\pm\boldsymbol{Q}}) h^-(t) + (\alpha^\dagger_{\pm\boldsymbol{Q}} + \beta_{\pm\boldsymbol{Q}}) h^+(t)], \tag{C1}$$

with $\lambda_{\pm\boldsymbol{Q}} = \zeta\frac{\sqrt{NS}}{4}(u_{\pm\boldsymbol{Q}} + v_{\pm\boldsymbol{Q}})$. As before, we are interested in the magnon Green's functions G_ν^R and $G_\nu^<$ for $\nu\in\{\alpha,\beta^\dagger\}$ and their corrections due to the external time-dependent pumping field. In order to do this, we consider the contour-ordered Green's function for the magnon ν, which, to second order in V, becomes

$$G_{\nu,\boldsymbol{q}}(t_1,t_2) = -i\langle \mathcal{T}_{\mathcal{C}}\nu_{\boldsymbol{q}}(t_1)\nu_{\boldsymbol{q}}^\dagger(t_2)e^{-i\int_{\mathcal{C}}dtV(t)}\rangle_0 \tag{C2}$$

$$= -i\langle \mathcal{T}_c\nu_{\boldsymbol{q}}(t_1)\nu_{\boldsymbol{q}}^\dagger(t_2)\rangle_0 - \left\langle \mathcal{T}_{\mathcal{C}}\int_{\mathcal{C}}dt\,\nu_{\boldsymbol{q}}(t_1)\nu_{\boldsymbol{q}}^\dagger(t_2)V(t)\right\rangle_0 + i\left\langle \mathcal{T}_{\mathcal{C}}\int_{\mathcal{C}}dtdt'\,\nu_{\boldsymbol{q}}(t_1)\nu_{\boldsymbol{q}}^\dagger(t_2)V(t)V(t')\right\rangle_0. \tag{C3}$$

Here, the angle brackets $\langle\cdots\rangle_0$ signify an average taken in the absence of V. The first-order term is clearly zero as it is odd in magnon operators. We consider the second-order term more closely:

$$i\left\langle \mathcal{T}_{\mathcal{C}}\int_{\mathcal{C}}dtdt'\,\nu_{\boldsymbol{q}}(t_1)\nu_{\boldsymbol{q}}^\dagger(t_2)V(t)V(t')\right\rangle_0 \tag{C4}$$

$$= 2i\sum_{\pm}\sum_{\pm'}\lambda_{\pm\boldsymbol{Q}}\lambda_{\pm'\boldsymbol{Q}}\left\langle \mathcal{T}_{\mathcal{C}}\int_{\mathcal{C}}dtdt'h^+(t')h^-(t)[\nu_{\boldsymbol{q}}(t_1)\nu_{\boldsymbol{q}}^\dagger(t_2)\nu_{\pm\boldsymbol{Q}}(t)\nu_{\pm'\boldsymbol{Q}}^\dagger(t')]\right\rangle \tag{C5}$$

$$= 2i\sum_{\pm}\sum_{\pm'}\lambda_{\pm\boldsymbol{Q}}\lambda_{\pm'\boldsymbol{Q}}\int_{\mathcal{C}}dtdt'h^+(t')h^-(t)[\langle \mathcal{T}_{\mathcal{C}}\nu_{\boldsymbol{q}}(t_1)\nu_{\pm'\boldsymbol{Q}}^\dagger(t')\rangle_0\langle \mathcal{T}_{\mathcal{C}}\nu_{\pm\boldsymbol{Q}}(t)\nu_{\boldsymbol{q}}^\dagger(t_2)\rangle_0$$

$$+ \langle \mathcal{T}_{\mathcal{C}}\nu_{\boldsymbol{q}}(t_1)\nu_{\boldsymbol{q}}^\dagger(t_2)\rangle_0\langle \mathcal{T}_{\mathcal{C}}\nu_{\pm\boldsymbol{Q}}(t)\nu_{\pm'\boldsymbol{Q}}^\dagger(t')\rangle_0], \tag{C6}$$

where we have done a Wick expansion and the second term in the expansion is zero. We have also extensively used the fact that the Hamiltonian in the absence of V is diagonal in α and $\beta^\dagger$, which allows us to discard several terms arising from the product V^2. The fact that the second term is zero can be seen as follows: Let us first define the quantity

$$\Sigma(t_1,t_2) = \langle \mathcal{T}_{\mathcal{C}}h^+(t_1)h^-(t_2)\rangle. \tag{C7}$$

We may then rewrite the second term in Eq. (C6) as

$$2i\sum_{\pm}\sum_{\pm'}\lambda_{\pm\boldsymbol{Q}}\lambda_{\pm'\boldsymbol{Q}}G^0_{\nu,\boldsymbol{q}}(t_1,t_2)\int_{\mathcal{C}}dtdt'\,\Sigma(t',t)G^0_{\nu,\pm\boldsymbol{Q}}(t,t')\delta_{\pm,\pm'} \tag{C8}$$

$$= -2i\sum_{\pm}\lambda^2_{\pm\boldsymbol{Q}}G^0_{\nu,\boldsymbol{q}}(t_1,t_2)\int_{\mathcal{C}}dt'\big(\Sigma\bullet G^0_{\nu,\pm\boldsymbol{Q}}\big)(t',t') \tag{C9}$$

$$= -2i\sum_{\pm}\lambda^2_{\pm\boldsymbol{Q}}G^0_{\nu,\boldsymbol{q}}(t_1,t_2)\bigg(\int_{-\infty}^{\infty}dt' + \int_{\infty}^{-\infty}dt'\bigg)\big(\Sigma\bullet G^0_{\nu,\pm\boldsymbol{Q}}\big)(t',t') = 0. \tag{C10}$$

Note that when multiplying out the term quadratic in the interaction V in Eq. (C3), we end up also with terms containing two α and two β magnon operators such that the Green's function correction in principle could depend on both kinds of magnons. It, however, also follows that since such terms have the same time structure as the second term in the Wick expansion, these terms are zero for the same reason as Eq. (C10).

We focus our attention now on the first term in the expansion and subtract the bare Green's function,

$$\Delta G^0_{\nu,\boldsymbol{q}}(t_1,t_2) = -2i\sum_{\pm}\sum_{\pm'}\lambda_{\pm\boldsymbol{Q}}\lambda_{\pm'\boldsymbol{Q}}\int_{\mathcal{C}}dtdt'\,\Sigma(t',t)G^0_{\nu,\pm'\boldsymbol{Q}}(t_1,t')G^0_{\nu,\pm\boldsymbol{Q}}(t,t_2)\delta_{\boldsymbol{q},\pm\boldsymbol{Q}}\delta_{\boldsymbol{q},\pm'\boldsymbol{Q}} \tag{C11}$$

$$= -2i\sum_{\pm}\delta_{\boldsymbol{q},\pm\boldsymbol{Q}}\lambda^2_{\pm\boldsymbol{Q}}\big(G^0_{\nu,\pm\boldsymbol{Q}}\bullet\Sigma\bullet G^0_{\nu,\pm\boldsymbol{Q}}\big)(t_1,t_2). \tag{C12}$$

In order to regain the real-time Green's functions, we utilize once again the Langreth rules. The commutator of the self-energy $\Sigma(t_1,t_2)$ is zero as it contains no operators, and thus, $\Sigma^{A/R}=0$, and $\Sigma^< = \Sigma$. It then follows that only the lesser component of the correction survives,

$$\Delta G^<_{\nu,\boldsymbol{q}}(t_1,t_2) = -2i\sum_{\pm}\delta_{\boldsymbol{q},\pm\boldsymbol{Q}}\lambda^2_{\pm\boldsymbol{Q}}\big(G^R_{\nu,\pm\boldsymbol{Q}}\circ\Sigma\circ G^A_{\nu,\pm\boldsymbol{Q}}\big)(t_1,t_2), \tag{C13}$$

where we have defined the circle product

$$(A\circ B)(t_1,t_2) = \int_{-\infty}^{\infty}dtA(t_1,t)B(t,t_2), \tag{C14}$$

using now the fact that $h^\pm(t) = e^{\mp i\Omega t} \Rightarrow \Sigma(t_1,t_2) = h_0^2e^{-i\Omega(t_1-t_2)}$. As both Σ and G^0_ν depend only on relative time, the circle product reduces to a regular convolution.

The Fourier transform of Σ is

$$\Sigma(\omega) = \int d(t_1-t_2)e^{i\omega(t_1-t_2)}e^{-i\Omega(t_1-t_2)}h_0^2 = 2\pi h_0^2\delta(\omega-\Omega). \tag{C15}$$

The second-order correction then becomes

$$\Delta G^{<}_{\nu,\boldsymbol{q}}(\omega) = -4\pi i h_0^2 \delta(\omega-\Omega)\sum_{\pm}\lambda^2_{\pm\boldsymbol{Q}}\left|G^R_\nu(\omega,\pm\boldsymbol{Q})\right|^2\delta_{\boldsymbol{q},\pm\boldsymbol{Q}}. \tag{C16}$$

If we now consider the definition of the distribution function

$$f^\nu(\omega,\boldsymbol{q}) = \frac{G^<_\nu(\omega,\boldsymbol{k})}{2i\mathrm{Im}\left\{G^R_\nu(\omega,\boldsymbol{k})\right\}} \tag{C17}$$

and the fact that to second order in the perturbation, only the lesser component of the correction survives, the distribution function is modified as follows:

$$f^\nu(\omega,\boldsymbol{q}) = n_B(\omega,T) - \frac{4\pi i h_0^2}{2i}\delta(\omega-\Omega)\left(\frac{-\eta^\nu}{\left(\omega-\omega^\nu_{\boldsymbol{q}}\right)^2+(\eta^\nu)^2}\right)^{-1}\sum_\pm \lambda^2_{\pm\boldsymbol{Q}}\frac{\delta_{\boldsymbol{q},\pm\boldsymbol{Q}}}{\left(\omega-\omega^\nu_{\pm\boldsymbol{Q}}\right)^2+(\eta^\nu)^2} \tag{C18}$$

$$= n_B(\omega,T) + \frac{2\pi h_0^2}{\eta^\nu}\delta(\omega-\Omega)\sum_\pm\lambda^2_{\pm\boldsymbol{Q}}\delta_{\boldsymbol{q},\pm\boldsymbol{Q}}. \tag{C19}$$

APPENDIX D: SPIN SUSCEPTIBILITY

In order to evaluate the spin current in Eq. (38), we need the retarded component of the spin susceptibility Green's function $G^R_{s^+}$, which follows from the imaginary-time Matsubara Green's function

$$\overline{G}^{\kappa\kappa'}_{s^+}(\tau_1,\tau_2,\boldsymbol{q}) = -\left\langle \mathcal{T}_\tau s^{\kappa'+}_{\boldsymbol{q}}(\tau_1)s^{\kappa-}_{\boldsymbol{q}}(\tau_2)\right\rangle_0 \tag{D1}$$

through the analytical continuation

$$G^{\kappa\kappa',R}_{s^+}(\omega,\boldsymbol{q}) = \overline{G}^{\kappa\kappa'}_{s^+}(i\omega_n\to\omega+i\eta,\boldsymbol{q}). \tag{D2}$$

The Fourier transformed Matsubara Green's function is defined by

$$\overline{G}^{\kappa\kappa'}_{s^+}(i\omega_n,\boldsymbol{q}) = \int_0^\beta d(\tau_1-\tau_2)\overline{G}^{\kappa\kappa'}_{s^+}(\tau_1,\tau_2,\boldsymbol{q})e^{i\omega_n(\tau_1-\tau_2)}, \tag{D3}$$

where $\omega_n = \frac{2\pi n}{\beta}$ are bosonic Matsubara frequencies.

We proceed by evaluating the imaginary-time Green's function in Eq. (D1) by inserting the explicit expression for the $s^\pm$ operators from Eq. (23). We also use the fact that for a Hamiltonian diagonal in a quantum number ν, e.g., the wave vector $\boldsymbol{k}$ as in the normal-metal Hamiltonian in Eq. (4), the time dependence of the operators $c^\dagger_{\boldsymbol{k},\sigma}$ and $c_{\boldsymbol{k},\sigma}$ follows from the Heisenberg equations and becomes

$$c^\dagger_{\boldsymbol{k},\sigma}(\tau) = e^{\xi_k\tau}c^\dagger_{\boldsymbol{k},\sigma}, \tag{D4a}$$

$$c_{\boldsymbol{k},\sigma}(\tau) = e^{-\xi_k\tau}c^\dagger_{\boldsymbol{k},\sigma}. \tag{D4b}$$

Using this, the imaginary-time Green's function becomes

$$\begin{aligned}
\overline{G}_{s^+}(\tau_1,\tau_2,\boldsymbol{q}) &= -\sum_{\boldsymbol{k}_1,\boldsymbol{k}_2}\left\langle T_\tau c^\dagger_{\boldsymbol{k}_1-\boldsymbol{q},\uparrow}(\tau_1)c_{\boldsymbol{k}_1^{\kappa'},\downarrow}(\tau_1)c^\dagger_{\boldsymbol{k}_2^\kappa,\downarrow}(\tau_2)c_{\boldsymbol{k}_2-\boldsymbol{q},\uparrow}(\tau_2)\right\rangle_0\\
&= -\sum_{\boldsymbol{k}_1,\boldsymbol{k}_2}\Big[\left\langle T_\tau c^\dagger_{\boldsymbol{k}_1-\boldsymbol{q},\uparrow}(\tau_1)c_{\boldsymbol{k}_1^{\kappa'},\downarrow}(\tau_1)\right\rangle_0\left\langle T_\tau c^\dagger_{\boldsymbol{k}_2^\kappa,\downarrow}(\tau_2)c_{\boldsymbol{k}_2-\boldsymbol{q},\uparrow}(\tau_2)\right\rangle_0 - \left\langle T_\tau \mathcal{T}_\tau c^\dagger_{\boldsymbol{k}_1-\boldsymbol{q},\uparrow}(\tau_1)c_{\boldsymbol{k}_2-\boldsymbol{q},\uparrow}(\tau_2)\right\rangle_0\\
&\quad\times\left\langle \mathcal{T}_\tau c^\dagger_{\boldsymbol{k}_2^\kappa,\downarrow}(\tau_2)c_{\boldsymbol{k}_1^{\kappa'},\downarrow}(\tau_1)\right\rangle_0\Big]\\
&= \sum_{\boldsymbol{k}_1,\boldsymbol{k}_2}\Big[\theta(\tau_1-\tau_2)\left\langle c^\dagger_{\boldsymbol{k}_1-\boldsymbol{q},\uparrow}c_{\boldsymbol{k}_2-\boldsymbol{q},\uparrow}\right\rangle_0\left\langle c_{\boldsymbol{k}_1^{\kappa'},\downarrow}c^\dagger_{\boldsymbol{k}_2^\kappa,\downarrow}\right\rangle_0 + \theta(\tau_2-\tau_1)\left\langle c_{\boldsymbol{k}_2-\boldsymbol{q},\uparrow}c^\dagger_{\boldsymbol{k}_1-\boldsymbol{q},\uparrow}\right\rangle_0\left\langle c^\dagger_{\boldsymbol{k}_2^\kappa,\downarrow}c_{\boldsymbol{k}_1^{\kappa'},\downarrow}\right\rangle_0\Big]\\
&\quad\times e^{(\xi_{k_1-q}-\xi_{k_1^{\kappa'}})\tau_1}e^{-(\xi_{k_2-q}-\xi_{k_2^\kappa})\tau_2}\\
&= \sum_{\boldsymbol{k}}\{\theta(\tau_1-\tau_2)n_F(\xi_{\boldsymbol{k}-\boldsymbol{q}},T)[1-n_F(\xi_{\boldsymbol{k}^\kappa},T)] + \theta(\tau_2-\tau_1)n_F(\xi_{\boldsymbol{k}^\kappa},T)[1-n_F(\xi_{\boldsymbol{k}-\boldsymbol{q}},T)]\}e^{(\xi_{k-q}-\xi_{k^\kappa})(\tau_1-\tau_2)},
\end{aligned} \tag{D5}$$

where n_F is the Fermi-Dirac distribution for fermions and T is temperature. Note that in the second line above, the first term vanishes as the normal-metal Hamiltonian is spin diagonal. We have also used the fact that the normal-metal Hamiltonian is diagonal in momentum, giving rise to δ_{k_1,k_2} and $\delta_{\kappa',\kappa}$ which simplify the expression. We now continue by Fourier transforming the Green's function,

$$\begin{aligned}\overline{G}_{s^+}(i\omega_n,\boldsymbol{q}) &= \int_0^\beta d(\tau_1-\tau_2)\overline{G}_{s^+}(\tau_1,\tau_2,\boldsymbol{q})e^{i\omega_n(\tau_1-\tau_2)}\\ &= -\sum_{\boldsymbol{k}} n_F(\boldsymbol{k}-\boldsymbol{q},T)[1-n_F(\boldsymbol{k}^\kappa,T)]\int_0^\beta d(\tau_1-\tau_2)e^{(i\omega_n+\xi_{\boldsymbol{k}-\boldsymbol{q}}-\xi_{\boldsymbol{k}^\kappa})(\tau_1-\tau_2)}\\ &= -\sum_{\boldsymbol{k}} n_F(\xi_{\boldsymbol{k}-\boldsymbol{q}},T)[1-n_F(\xi_{\boldsymbol{k}^\kappa},T)]\frac{e^{\beta(\xi_{\boldsymbol{k}-\boldsymbol{q}}-\xi_{\boldsymbol{k}^\kappa})}-1}{i\omega_n+\xi_{\boldsymbol{k}-\boldsymbol{q}}-\xi_{\boldsymbol{k}^\kappa}}\\ &= \sum_{\boldsymbol{k}}\frac{n_F(\xi_{\boldsymbol{k}-\boldsymbol{q}},T)-n_F(\xi_{\boldsymbol{k}^\kappa},T)}{i\omega_n+\xi_{\boldsymbol{k}-\boldsymbol{q}}-\xi_{\boldsymbol{k}^\kappa}}.\end{aligned} \tag{D6}$$

It then follows that the retarded spin susceptibility Green's function is given by

$$G^R_{s^+,\kappa\kappa'}(\omega,\boldsymbol{q}) = \delta_{\kappa,\kappa'}G^R_{s^+,\kappa}(\omega,\boldsymbol{q}) = \delta_{\kappa,\kappa'}\sum_{\boldsymbol{k}}\frac{n_F(\xi_{\boldsymbol{k}-\boldsymbol{q}},T)-n_F(\xi_{\boldsymbol{k}^\kappa},T)}{\omega+\xi_{\boldsymbol{k}-\boldsymbol{q}}-\xi^\kappa_{\boldsymbol{k}}+i\eta^N}. \tag{D7}$$

[1] A. Hirohata, K. Yamada, Y. Nakatani, L. Prejbeanu, B. Diény, P. Pirro, and B. Hillebrands, J. Magn. Magn. Mater. **509**, 166711 (2020).

[2] Y. Tserkovnyak, A. Brataas, and G. E. W. Bauer, Phys. Rev. B **66**, 224403 (2002).

[3] Y. Tserkovnyak, A. Brataas, G. E. W. Bauer, and B. I. Halperin, Rev. Mod. Phys. **77**, 1375 (2005).

[4] Y. Tserkovnyak, A. Brataas, and G. E. W. Bauer, Phys. Rev. Lett. **88**, 117601 (2002).

[5] R. Cheng, J. Xiao, Q. Niu, and A. Brataas, Phys. Rev. Lett. **113**, 057601 (2014).

[6] S. Takei, T. Moriyama, T. Ono, and Y. Tserkovnyak, Phys. Rev. B **92**, 020409(R) (2015).

[7] K.-H. Ahn, A. Hariki, K.-W. Lee, and J. Kuneš, Phys. Rev. B **99**, 184432 (2019).

[8] S. Hayami, Y. Yanagi, and H. Kusunose, J. Phys. Soc. Jpn. **88**, 123702 (2019).

[9] L. Šmejkal, R. González-Hernández, T. Jungwirth, and J. Sinova, Sci. Adv. **6**, eaaz8809 (2020).

[10] L.-D. Yuan, Z. Wang, J.-W. Luo, E. I. Rashba, and A. Zunger, Phys. Rev. B **102**, 014422 (2020).

[11] L. Šmejkal, J. Sinova, and T. Jungwirth, Phys. Rev. X **12**, 031042 (2022).

[12] L. Šmejkal, J. Sinova, and T. Jungwirth, Phys. Rev. X **12**, 040501 (2022).

[13] I. I. Mazin, Phys. Rev. B **107**, L100418 (2023).

[14] Q. Cui, B. Zeng, P. Cui, T. Yu, and H. Yang, Phys. Rev. B **108**, L180401 (2023).

[15] B. Brekke, A. Brataas, and A. Sudbø, Phys. Rev. B **108**, 224421 (2023).

[16] O. Fedchenko *et al.*, Sci. Adv. **10** (2024).

[17] L. Šmejkal, A. Marmodoro, K.-H. Ahn, R. Gonzalez-Hernandez, I. Turek, S. Mankovsky, H. Ebert, S. W. D'Souza, O. Šipr, J. Sinova, and T. Jungwirth, Phys. Rev. Lett. **131**, 256703 (2023).

[18] A. Hariki, T. Yamaguchi, D. Kriegner, K. W. Edmonds, P. Wadley, S. S. Dhesi, G. Springholz, L. Šmejkal, K. Výborný, T. Jungwirth, and J. Kuneš, Phys. Rev. Lett. **132**, 176701 (2024).

[19] T. Kato, Y. Ohnuma, M. Matsuo, J. Rech, T. Jonckheere, and T. Martin, Phys. Rev. B **99**, 144411 (2019).

[20] J. Rammer and H. Smith, Rev. Mod. Phys. **58**, 323 (1986).

[21] G. Stefanucci and R. Van Leeuwen, *Nonequilibrium Many-Body Theory of Quantum Systems: A Modern Introduction* (Cambridge University Press, Cambridge, 2013).

[22] A. Kamra and W. Belzig, Phys. Rev. Lett. **119**, 197201 (2017).

[23] E. H. Fyhn and J. Linder, Phys. Rev. B **103**, 134508 (2021).

[24] C. Sun and J. Linder, Phys. Rev. B **108**, L140408 (2023).